A Study of Transient Dynamics with Frictional Contact: Oblique Elastic Impact of Spheres

Philip P. Garland and Robert J. Rogers

Department of Mechanical Engineering
University of New Brunswick
Fredericton, N.B., Canada

Abstract: *Oblique elastic impact of spheres and the related case for cylinders have been studied cases for many years in simulations of systems with loose supports, such as heat exchanger tube-support interaction, as well as granular flows and robotic task modeling. The problem is a relative simple one in the class of transient frictional contact problems in that the stresses away from the contact zone are typically neglected. The available continuum model solutions from literature show some very interesting features. For near normal angles of incidence, these solutions combine a Hertzian contact stress solution in the normal direction with a partial-slip shear stress distribution in the tangential direction, in which a central portion of the contact zone is sticking while the coincident points of the outer annulus slide relative to one another. Both stress distributions change rapidly over the impact duration. The partial-slip shear stress distribution is caused by the simultaneous inclusion of tangential compliance and friction effects, and gives rise to tangential force reversal prior to the loss of contact. Initial investigations using the penalty contact formulation in Abaqus/Explicit™ v. 6.7 show some very interesting results. Both the normal and shear stress results show smooth distributions, however the shear stress distributions show an unexpected antisymmetry. Nevertheless, the Abaqus/Explicit™ solution is able to capture the essential features of tangential force oscillation predicted by continuum models.*

Keywords: *Oblique elastic impact, friction, explicit dynamics, penalty contact.*

1. Introduction

Engineers commonly turn to finite element analysis to handle contact problems due to the difficulty of determining the interactions within the contact zone of the contacting bodies. This difficulty is caused by lack of available analytical solutions, particularly in the presence of friction, and the possibility of changes to the geometric configuration of the bodies in response to the contact forces, particularly in the transient dynamic solution of vibration dominated systems.

The formulation approach taken in finite element contact analysis is quite different than the analytical formulation of these problems (Laursen, 2002). Therefore, finite element formulations can lead to solutions that are independent of the assumptions common to continuum-based analytical solutions. Again, the lack of analytical solutions makes it difficult to evaluate the correctness of the finite element results in some cases. This fact accepted, however, it is not unreasonable to expect finite element solutions of relatively simple problems, even with complex interactions such as those introduced by friction, to match continuum based solutions.

The case of oblique elastic impact of two spheres has all of the prerequisites for testing such agreement between finite element and analytically-based solutions. Firstly, the expected contact zone geometry is a relatively simple one. The solution of the interaction in the direction normal to the colliding sphere is well known, and the normal stress distributions can be obtained from well-established Hertzian contact theory. Inclusion of friction provides a complex surface interaction in the tangential direction that, when combined with tangential compliance effects, makes the problem nontrivial. Finally, there are several analytically-based solutions for the shear stress distributions during impact (Maw et al., 1976; Jaeger, 1992; Garland and Rogers, 2008a). These continuum model solutions utilize a constant coefficient of friction definition.

The available continuum model solutions show tangential force reversal during the impact duration for certain near normal angles of incidence. These solutions have shown that at certain points during impact, the coincident points on the impacting spheres can be in full sticking – with all coincident points in the contact zone sticking together –, full sliding – with all coincident points having some relative tangential slip –, or partial-slip – with coincident points in the central portion of the contact zone sticking together while those in the outer annulus of the contact zone have some relative slip. These different possibilities of surface interaction lead to shear stress distributions that are constantly evolving during impact. The presence of the different characteristic shear stress distribution types for any given impact is dependent on incidence angle, so that all three characteristic types could be seen at different times during the impact or only one type could persist throughout. These continuum models consider the localized deformation effects only and assume that the normal and shear stress distributions are smooth functions.

Although there is a large body of literature on contact formulation and specific examples analyzed using finite element methods, a relatively small amount of literature is directly relevant to this problem. The first apparent specific treatment of the classic Hertzian contact problem with finite elements was performed by Chandrasekaran et al. (1987). They considered the case of normal static loading of two cylinders in contact with varying amounts of friction. The method used for the solution is known as a penalty formulation in which a load step applied to the pseudo equilibrium configuration enforces the compatibility condition. Relative magnitudes of normal and tangential nodal forces are then used to determine the frictional contact conditions. Reasonable agreement is achieved for nodal force values at the contact interface between the analytical solution and numerical solution presented.

Lim and Stronge (1999) considered the case oblique impact of a rigid cylinder and an elastic-plastic half-space. Their analysis was based on a lumped parameter formulation that used a constant ratio of tangential to normal compliance in the contact zone. Although much of the analysis does not apply to our case, comparison is made to a DYNA2D™ finite element model of the same problem. As it is secondary to the work presented, little information is given as to the exact contact formulation used in the finite element model. However, comparison of the elastic impact case for both models show reasonable agreement of the tangential force waveforms. It should be noted that the lumped parameter model does show some slight differences when compared to an elastic continuum model (Garland and Rogers, 2008b). Unfortunately, the shear stress distributions during impact are not shown (Lim and Stronge, 1999).

Jaeger (2001) presented results of a 2-D finite element model of a rigid cylinder in contact with an elastic half-space obtained using the commercially available finite elements package Ansys™. In this model, a normal load is first applied to the rigid punch and then the tangential load is applied in three increasing steps, all of which are less than that expected for full sliding. The results of the finite element model, which employs a Lagrangian multiplier method to define the contact conditions, compare very well with the results obtained from Jaeger's previous algorithm (Jaeger, 1992). The one notable difference is the slight asymmetry in the shear distributions which is present in the finite element solution but absent from the analytical solution. This difference is attributed to the fact that the analytical solution assumes that the contact surface remains planar.

Wu et al. (2003) investigated the results of incidence angle on velocity-based normal and tangential coefficients of restitution values for elastic and elastic-plastic oblique impacts analyzed using the DYNA3D™ code. The finite element model employed a rigid 3D sphere impacting an elastic half-space. For the elastic impacts, the coefficient of normal restitution remained at unity for all angles. The coefficient of tangential restitution varied from about 0.95 at 85° to normal (i.e., glancing impact) to a value of 0.75 at near normal incidence angles, with a minimum of around 0.6 at 45°.

The plastic impact simulations were performed using both a rigid sphere impacting an elastic-perfectly plastic half-space and elastic-perfectly-plastic sphere impacting a rigid half-space. Interestingly, the results for both the normal and tangential coefficients of restitution are quite different for these two cases. Wu et al. (2003) also present a comparison of the rebound vs. incidence angle results for their model to previous experimental studies [Maw et al., 1981; Kharaz et al., 2001) and numerical models [Maw et al, 1976; Thornton and Zhang, 2001]. These comparisons show very reasonable agreement. The results given do not include surface stress distributions.

This paper presents the contact forces and surface stress results of a finite element model of a sphere impacting a rigid plate at various angles of obliquity. The 3D finite element model was formulated using Abaqus/Explicit™ v. 6.7. Comparisons of the results are made to those of an equivalent continuum model simulation.

2. Finite element model

The geometry of the finite element model can be seen in Fig.1. Instead of modeling two deformable spheres, the finite element model replaces one of the spheres with a rigid plate to reduce the computational effort. Since the contact zone remains circular, the analysis is equivalent to modeling impact of an unconstrained sphere with a fixed sphere. Impacts of the sphere against the rigid plate at various incidence angles were simulated using the explicit dynamic formulation of Abaqus/Explicit™. The sphere was discretized using around 62,000 modified formulation tetrahedral elements with the mesh being heavily biased towards the contact zone. The rigid plate was modeled using 40,000 rigid quadrilateral elements. This high number of elements allowed for very fine resolution of the stress distributions.

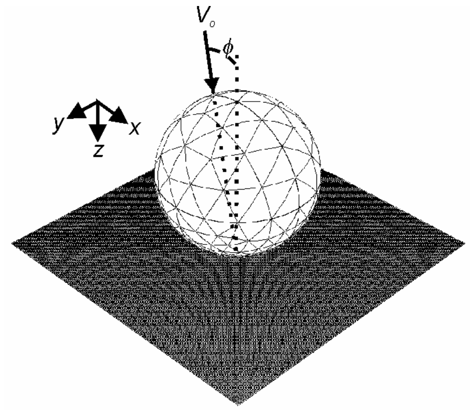

Figure 1. Finite element model geometry.

The analysis was performed using the general contact algorithm in Abaqus/Explicit™ (Abaqus Analysis User's Manual, 2007). The penalty contact formulation was used for both normal and tangential interactions between the sphere (slave surface) and rigid plate (master surface). In the starting position, the sphere and plate had a small gap between them in order to avoid the difficulties of overlapping. To begin the analysis, the sphere was imparted with some initial velocity limited to the *xz*-plane (i.e., $V_{yo} = 0$). This velocity was unrealistically high in order to produce deformations large enough to allow for the stress distributions to be analyzed. Since the material definition for the sphere did not include any plasticity information, the impact remained elastic even though unrealistically high force values were reached.

The test case used a 200 mm diameter steel ($E = 206 \times 10^9$ Pa, $\nu = 0.3$, $\rho = 7800$ kg/m^3) sphere, with a coefficient of friction of 0.2. The normalized incidence angles analyzed were the same as those used in the continuum model, namely $\psi = 0.2, 0.5, 1.2, 2.0, 3.0,$ and 4.0. These incidence angles were normalized by (Maw et al., 1976)

$$\psi = \frac{2(1-\nu)}{\mu(2-\nu)}\tan\phi \tag{1}$$

where μ is the friction coefficient, ν is Poisson's ratio and ϕ is the physical incidence angle measured from normal.

With the normalized incidence angle thus defined, Maw et al. (1976) categorize the oblique impact based on expected surface behaviour at initial contact. For $\psi < 1$, the impact begins with full sticking of coincident points. As the impact progresses, the tangential force increases to some maximum value that is less than the limiting friction envelope[1] before reversing direction. For

[1] Under an assumption of a constant coefficient of friction, the tangential force is limited to the product of the current normal force and the friction coefficient, where there is relative sliding of coincident points in the contact zone. For reversed sliding (i.e., sliding in the direction opposite to the initial tangential velocity), the tangential force is equal to the negative of this product.

certain angles, the impact will end with full reversed sliding, in which the tangential force is equal to the negative of the limiting friction envelope. This is called the low incidence angle regime.

For $1 \le \psi < 4\chi$-1, the impact begins with full sliding and the tangential force is given by the current friction envelope value. The dimensionless parameter, χ, incorporates the mass moment of inertia of the colliding sphere, I, and is defined by

$$\chi = \frac{(1-\nu)\left(1+\left(\frac{1}{K}\right)^2\right)}{2-\nu}; \qquad K = \left(\frac{I}{mR^2}\right)^{1/2} \tag{2}$$

where m is the mass of the sphere and R is the sphere's radius.

In this intermediate incidence angle range, the tangential force leaves the friction envelope at some point during impact and then reverses direction. Again, the impact ends with reversed sliding. For $\psi \ge 4\chi$-1, full sliding persists throughout the impact duration. In this case, the tangential force is equal to the limiting friction envelope for the entirety of impact. This is the high incidence angle regime.

The continuum model used a fixed time step of 0.2 μsec while the finite element model used an automatic time step. History and field data of the finite element model were printed to the output database file at every 0.2 μsec of the simulation. For both simulations, the initial velocity in the normal direction was held constant at 100 m/s; the tangential velocity was adjusted to provide the proper incidence angle. This gave initial conditions of

$$V_{zo} = 100 \ \mathrm{m}/s\,; \qquad V_{xo} = V_{zo} \tan\phi \tag{3}$$

3. Results and comparison to continuum model

The specifics of the continuum model method used for the comparison presented in this section can be seen in a recent paper (Garland and Rogers, 2008a). Comparisons of the stress distributions of both methods are limited to graphical presentations; comparisons of the normal and tangential force waveform results for the two solutions are given graphically and compared using the coefficient of determination defined by

$$R^2 = 1.0 - \frac{\sum_{i=1}^{N}\left(Y_i^{/} - Y_i\right)^2}{\sum_{i=1}^{N}\left(Y_i^{/} - \overline{Y}^{/}\right)^2} \tag{4}$$

where Y'_i is the result obtained from the continuum model simulation, $\bar{Y}'$ is the mean value over the full impact duration of these results, and Y_i is the similar result of the finite element method.

Figures 2 (a) through (l) show the normal (z-axis) force and tangential (x-axis)force waveforms of both the finite element and continuum models. The tangential force waveforms in the y-axis direction showed near zero force levels and are not included in these figures. In all cases, the maximum normal force obtained from the continuum model is somewhat less than that of the finite element model. The impact duration of the continuum model simulations is somewhat longer than the finite element model simulations.

The tangential force waveforms obtained from the finite element model of Fig. 2 show force direction reversal during the impact duration with the exception of the $\psi = 4.0$ case. The tangential force waveforms show a degree of waviness for $\psi = 0.2$ and 0.5 that is not present in the other cases. The maximum and minimum force results of the two methods are slightly different, with bigger differences in the minimum values. Also, the times of tangential force reversal are slightly different for the two methods.

Table 1 shows the comparison of several impact parameters from the two methods. As expected, the continuum model simulations have identical impact durations and identical maximum normal forces because the initial normal velocity is the same for all incidence angles. Somewhat surprisingly, the different incidence angles of the finite element simulations show slightly different impact durations and maximum normal forces with no discernable pattern. The maximum normal force values obtained from the two methods show differences of 10.2 % to 13.6 %; the impact duration results of the finite element simulations vary from -5.6 % to -8.2 % difference from the continuum model simulations.

The maximum tangential force results vary between the continuum model method and the finite element simulation by -2.5 % to 13.4 %. The minimum tangential forces show that the finite element solutions are significantly lower than the continuum model simulations, with percent differences from -42.7 % to -95.0 %. This higher percent difference is due to the relatively low magnitude of the minimum forces. The R^2 values of the normal force waveform comparisons are 0.893, 0.837, 0.896, 0.903, 0.909, and 0.910 for normalized incidence angles 0.2, 0.5, 1.2, 2.0, 3.0, and 4.0, respectively. Comparison of the tangential force waveforms gives R^2 values of 0.839, 0.836, 0.842, 0.930, 0.945, and 0.949 for normalized incidence angles 0.2, 0.5, 1.2, 2.0, 3.0, and 4.0, respectively.

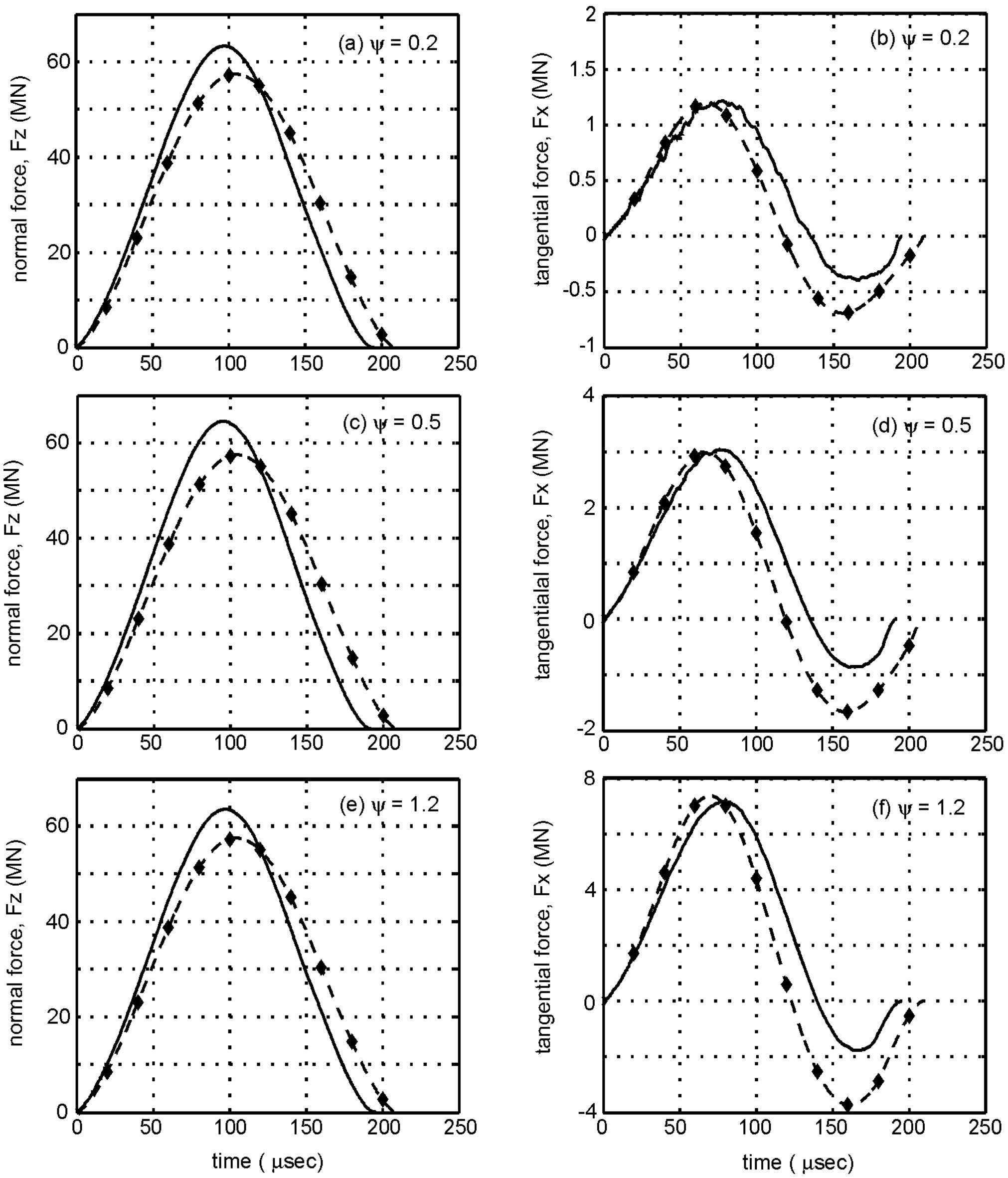

Figure 2. Normal and tangential force waveforms at indicated incidence angles. (Continuum model – dashed with diamonds; Finite element model – solid) (Normal force – left side; Tangential force – right side)

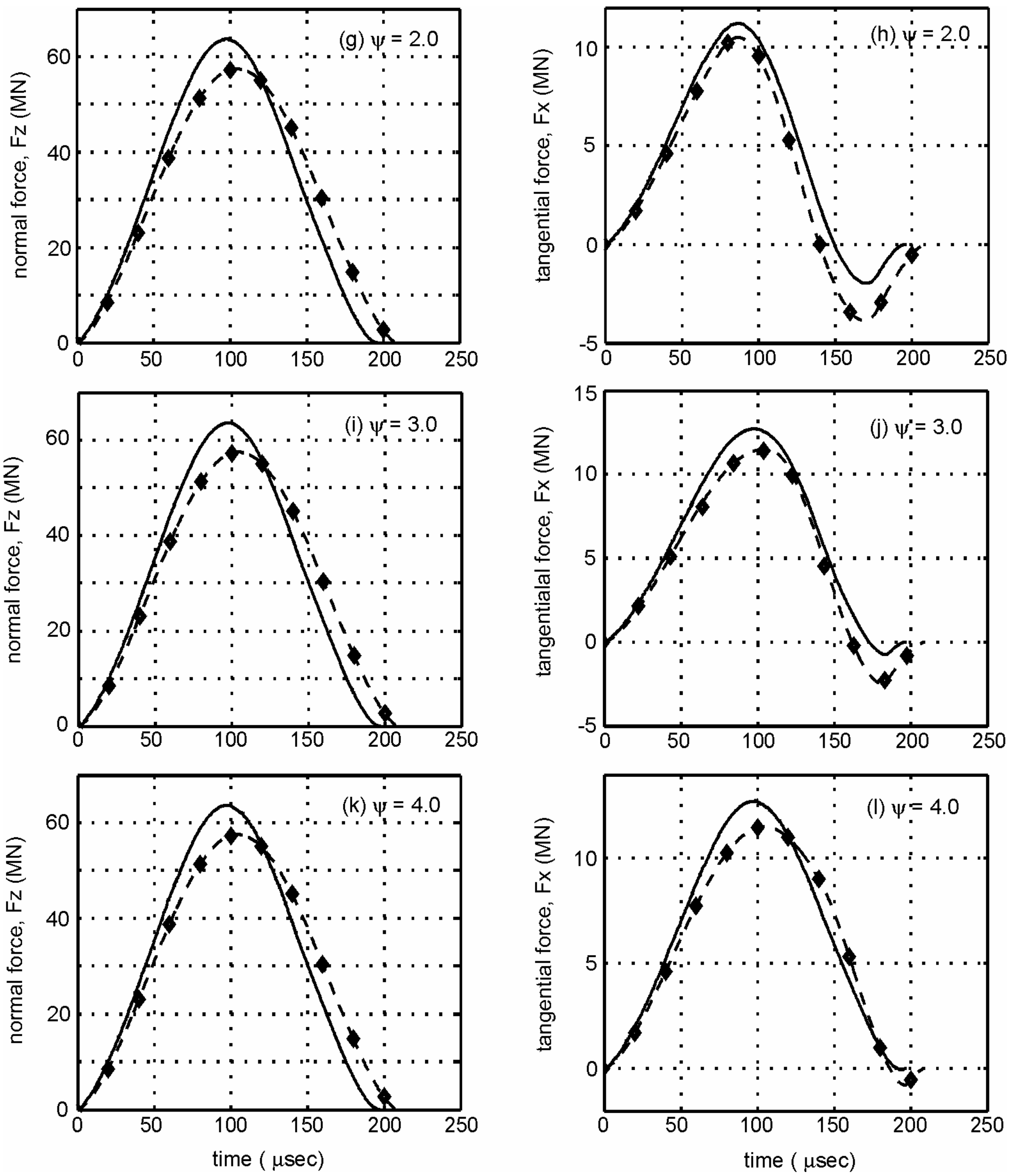

Figure 2. Normal and tangential force waveforms at indicated incidence angles – cont'd. (Continuum model – dashed with diamonds; Finite element model – solid) (Normal force – left side; Tangential force – right side)

Table 1. Comparison of impact force parameter results.

Angle	Maximum normal force (MN)			Maximum tangential force (MN)			Minimum tangential force (MN)			Impact duration (μsec)		
	Cont	**F.E.**	**% Diff**	**Cont**	**F.E.**	**% Diff**	**Cont**	**F.E.**	**% Diff**	**Cont**	**F.E.**	**% Diff**
0.2	57.5	63.4	10.2	1.19	1.22	2.4	-0.69	-0.39	-42.7	209.2	195.0	-6.7
0.5	57.5	64.5	12.3	2.99	3.04	1.7	-1.66	-0.87	-47.8	209.2	192.0	-8.2
1.2	57.5	63.5	10.6	7.35	7.17	-2.5	-3.72	-1.76	-52.7	209.2	195.4	-6.6
2.0	57.5	63.7	10.8	10.5	11.2	6.9	-3.86	-1.97	-49.0	209.2	196.4	-6.1
3.0	57.5	63.7	10.7	11.5	12.7	10.6	-2.46	-0.74	-69.9	209.2	197.4	-5.6
4.0	57.5	65.3	13.6	11.5	13.0	13.4	-0.77	-0.04	-94.9	209.2	197.4	-5.6
Avg % diff. ± std. dev.			11.4 ± 1.3			5.4 ± 6.0			-59.5 ± 19.7			-6.5 ± 1.0

It is difficult to predict the trends in tangential force with incidence angle without proper normalization of these waveforms. In order to normalize the force results, the force values are divided by the product of the friction coefficient and maximum normal force, and the time scales are divided by the impact duration, τ. The normalized force waveforms, both normal and tangential, obtained from both solutions are shown in Figs. 3 (a) through (f). From these figures, one can see that the normal force waveforms show better agreement. The normalized tangential force waveforms show less agreement than the raw waveforms from which they were derived.

In all cases, the time of tangential force reversal occurs much earlier in the impact duration for the continuum model results than for the finite element results. Somewhat interesting is the fact that the finite element result of the tangential force waveform for $\psi = 1.2$ does not lie on the friction envelope at the beginning of impact as one would expect. The finite element tangential force results at higher incidence angles do begin impact in the full sliding interface condition. Full sliding appears to persist throughtout the impact duration for the $\psi = 4.0$ case of the finite element results.The corresponding case for the continuum model shows definite tangential force reversal.

The R^2 values for the normalized normal force waveforms are 0.993, 0.992, 0.993, 0.992, 0.991, and 0.984 for incidence angles 0.2, 0.5, 1.2, 2.0, 3.0, and 4.0, respectively. These values show improved agreement compared to the raw normal force waveforms and indicate almost perfect agreement between the normalized normal force waveforms of the two solutions. For the normalized tangential force waveforms, the R^2 values are 0.706, 0.686, 0.722, 0.861, 0.911, and 0.979 for incidence angles 0.2, 0.5, 1.2, 2.0, 3.0, and 4.0, respectively. These values indicate less agreement between the normalized tangential waveforms than the raw tangential waveforms.

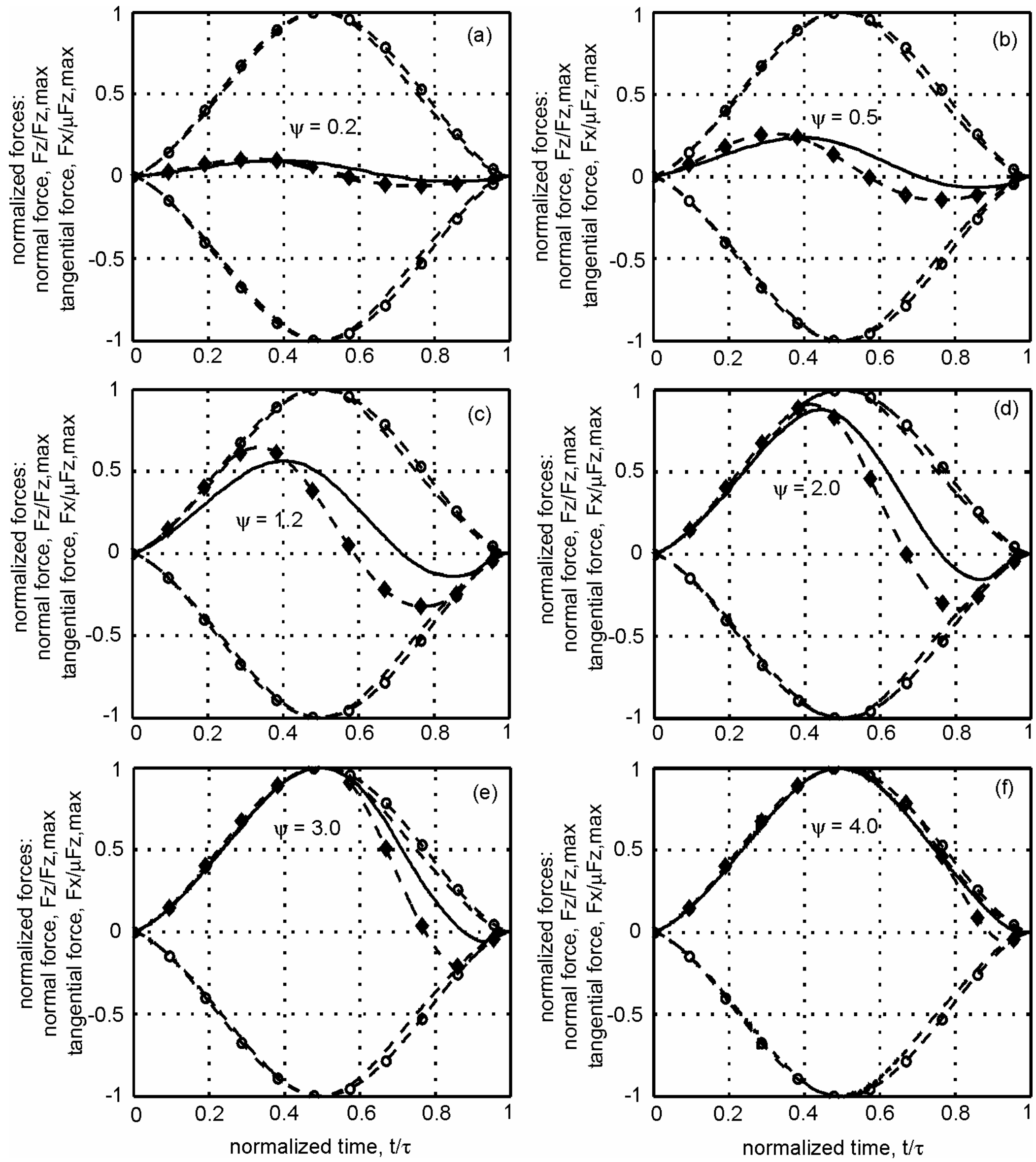

Figure 3. Normalized force waveforms at indicated incidence angles.
(Continuum model tangential – dashed with diamonds;
Finite element tangential – solid;
Continuum model normal – dashed with circles; Finite element normal – dashed)

Figures 4 (a) and (b) show the normalized normal stress distribution (CPRESS) at maximum compression for a normalized incidence angle of 0.5 obtained from the finite element and continuum model solutions, respectively. The normal stress distributions obtained from the two solutions are quite similar; both solutions give smooth normal stress distributions of similar size and shape.

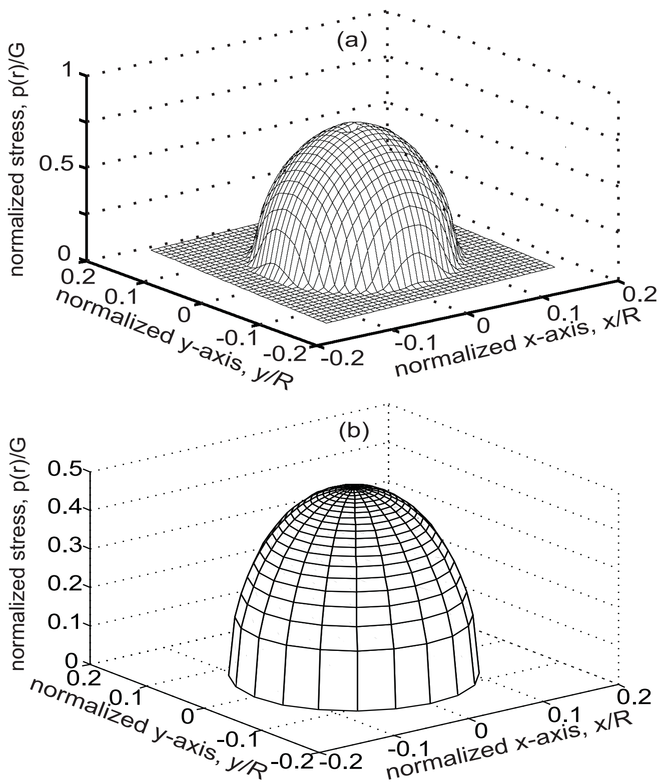

Figure 4. Normalized normal stress distribution at maximum compression (t/τ = 0.5) for ψ = 0.5. (a) Finite element result; and (b) Continuum model result.

In order to more closely examine the results of the two solutions, Fig. 5 shows the normalized normal stress distribution along the center line ($y = 0$) of both solutions. This figure shows that the continuum model solution for normal stress along the center line has a smaller maximum value than the finite element result. The contact areas of the two solutions can be seen to be in very good agreement. The finite element results exhibit an odd dip in value at around the center of the contact zone, but the overall agreement of the two stress distributions is very reasonable. These results are typical of results obtained at other times of the impact duration and for other incidence angles.

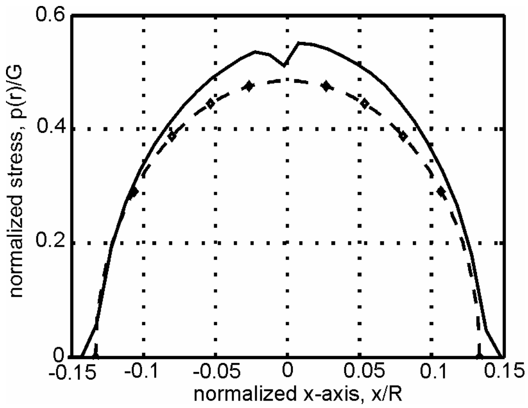

Figure 5. Normalized normal stress distribution along centerline (y = 0). (Continuum model – dashed with diamonds; Finite element – solid)

The corresponding normalized shear stress distributions in the x-axis direction of the finite element and continuum models are shown in Figs. 6 (a) and (b). The Abaqus™ results were obtained from the CSHEAR1 data of the rigid plate nodes. The distribution of the continuum model simulation does not resemble the finite element solution, which contains an approximate antisymmetry about the center line (x = 0) of the contact zone. This antisymmetry, which results in part of the shear distribution being negative while the other portion is positive, could be caused by the radially symmetric frictional shear stress distribution expected to be present in the absence of a tangential load. This frictional distribution is not considered in the continuum model because it has no net effect (i.e., sums to zero).

Plotting the shear stress distributions along the center line, as in Fig. 7, shows the large difference between the continuum and finite element model solutions. The one similar feature between the two methods is, once again, the contact area. The continuum model and finite element solutions result in similar net tangential force waveforms, even though the shear stress results obtained from the two methods are quite different.

The normalized shear stress distribution for the y-axis direction (CSHEAR2) obtained from the finite element simulation is plotted in Fig. 8. This shear stress distribution exhibits the same antisymmetric behavior as the results for the shear stress in the x-axis direction. The actual levels of shear stress in the y-axis direction are on the same order of magnitude as those in the x-axis direction. This result is quite interesting since the net tangential force in the y-axis during impact was very close to zero, which indicates that the shear stress in the y-axis direction sums to approximately zero. The continuum model assumes that the shear stress distribution is everywhere zero in the y-axis direction. The nonzero shear stress distribution in the y-axis direction may be further evidence of the presence of a radially symmetric frictional distribution, especially considering that the y-axis stress is of a similar magnitude as the x-axis stress.

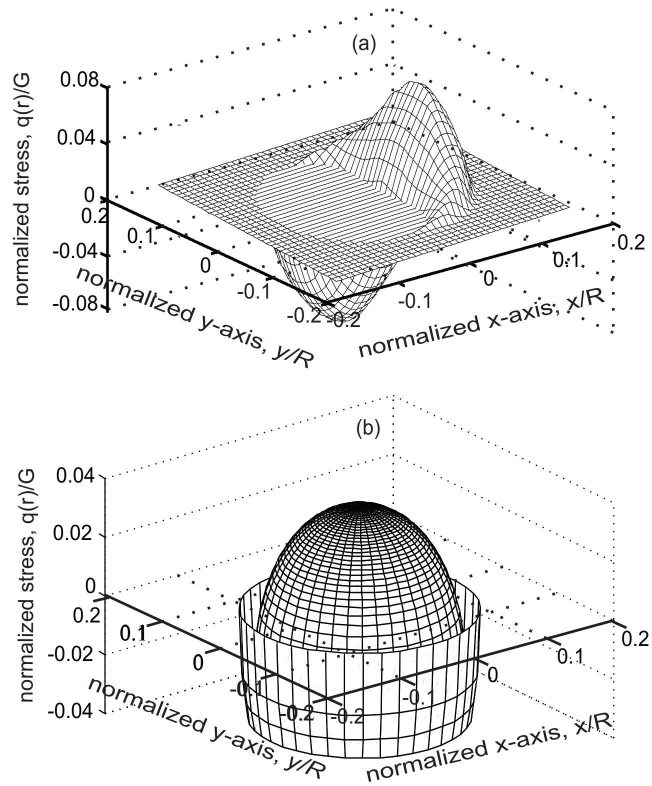

Figure 6. Normalized shear stress distribution at maximum compression (t/τ = 0.5) for ψ = 0.5. (a) Finite element result; and (b) Continuum model result.

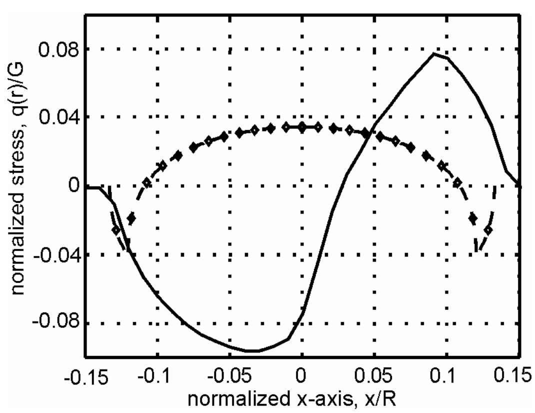

Figure 7. Normalized shear stress distribution along centerline (y = 0). (Continuum model – dashed with diamonds; Finite element – solid)

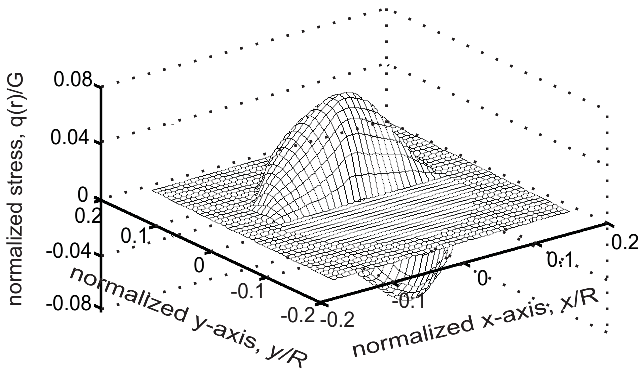

Figure 8. Finite element results for normalized shear stress in the y-axis direction at maximum compression (t/τ = 0.5) for ψ = 0.5.

4. Conclusions

In theory, the finite element method offers a solution to the oblique impact problem that is free of the shortcomings and assumptions of the continuum models. The finite element model should be capable of handling bodies of arbitrary geometry with no limitation on the shape of contact zone. It should also provide solutions for any loading scenario including plastic loading. The finite element method is subject to its own algorithmic assumptions, however, which include the method of contact formulation and time-stepping dynamic simulation.

The normal stress distributions obtained by the finite element simulations showed reasonable agreement with the results obtained from continuum model simulations. The shear stress results in both x-axis and y-axis directions obtained from the finite element models showed antisymmetric distributions that do not agree with the continuum model predictions. These shear stress results were quite curious given the reasonable agreement of the tangential force waveforms, but could be due to a radially symmetric frictional shear stress that has no net effect on the tangential force.

Comparisons showed reasonable agreement between the normal and tangential force waveforms obtained from the two methods. When the force waveforms of the finite element and continuum model simulations were normalized, the agreement between the normal force waveforms improved dramatically. On the other hand, the normalized tangential force waveforms do not agree as well as the raw tangential force waveforms did. In general, the normalized finite element results show that the time of tangential force reversal is later than that of the continuum model at similar incidence angles. The critical angles for initial sliding on incidence and full sliding throughout the impact duration obtained from the finite element solution did not quite match the values of these angles predicted by theory. Also, the impact durations for the finite element simulations were somewhat shorter (average 6.5%) than for the continuum model simulations.

Even with the differences between the two solutions, the finite element results did show the essential features of tangential force reversal predicted by continuum models. These results are curious given the large differences in the surface shear stress results between the finite element model and those expected. Simulation of the problem presented with an implicit dynamic formulation using Abaqus/Standard™, as well as development of a continuum model that includes the possible radially symmetric frictional shear stress, are the subjects of further research.

References

1. Abaqus Analysis User's Manual v6.7, Online Documentation, Simulia Inc. 2007.
2. Chandrasekaran, N., Haisler, W.E., and Goforth, R.E., "Finite Element Analysis of Hertz Contact Problems with Friction," Finite Element in Analysis and Design, vol. 3, pp.477-495, 1987.
3. Garland, P.P., and Rogers, R.J., "An Analytical Solution for Shear Stress Distributions during Oblique Elastic Impact of Similar Spheres," ASME Journal of Computational and Nonlinear Dynamics, vol.3, pp. 011002-1 – 011002-9, 2008a.
4. Garland, P.P., and Rogers, R.J., "A Comparison of Macroscopic Modelling Approaches for Oblique Impact," to be presented at CSME conference 2008, Ottawa, June 5-8, 2008b.
5. Jaeger, J., "Elastic Impact with Friction," Ph.D. Thesis, Delft University, 1992.
6. Jaeger, J., "New Analytic Solutions for a Flat Rounded Punch Compared with FEM," Contact Mechanics V, WIT Press, pp. 307-316, 2001.
7. Kharaz, A.H., Gorham, D.A., and Salman, A.D., "An Experimental Study of the Elastic Rebound of Spheres," Powder Technology, vol. 120, pp. 281-291, 2001.
8. Laursen, T.A., "Computational Contact and Impact Mechanics: Fundamentals of Modeling Interfacial Phenomena in Nonlinear Finite Analysis," Springer, Berlin, 2002.
9. Lim, C.T., and Stronge, W.J., "Oblique Elastic-Plastic Impact between Rough Cylinders in Plane Strain," International Journal of Engineering Science, vol. 37, pp. 97-122, 1999.
10. Maw, N., Barber, J.R., and Fawcett, J.N., "Oblique Impact of Elastic Spheres," Wear, vol. 38, pp. 101-114, 1976.
11. Maw, N., Barber, J.R., and Fawcett, J.N., "The Role of Elastic Tangential Compliance in Oblique Impact," ASME Journal of Lubrication Technology, vol. 103, pp. 74-80, 1981.
12. Thornton, C., and Zhang, L., "A DEM Comparison of Different Shear Testing Devices," Proceedings of the 4th International Congress on the Micromechanics of Granular Materials, Sendai, Japan, pp. 183-190, 2001.
13. Wu, C.Y., Li, L.Y., and Thornton, C., "Rebound Behaviour of Spheres for Plastic Impacts," International Journal of Impact Engineering, vol. 28, pp. 929-946, 2003.

Acknowledgements

The authors thank the Natural Sciences and Engineering Research Council of Canada for funding this research and the reviewers of this paper who made some useful suggestions to improve the quality of the results.